Reduction of native singly ionized zinc vacancies content by 2.5 MeV electron irradiation of ZnGeP_2 single crystals

Charlotte Vernozy, Antonino Alessi, Johan Petit, Audrey Courpron, Olivier Cavani, Valérie Véniard

▶ **To cite this version:**

Charlotte Vernozy, Antonino Alessi, Johan Petit, Audrey Courpron, Olivier Cavani, et al.. Reduction of native singly ionized zinc vacancies content by 2.5 MeV electron irradiation of ZnGeP_2 single crystals. Physica Status Solidi A (applications and materials science), 2024, 221 (11), pp.2300818. 10.1002/pssa.202300818 . hal-04661164

HAL Id: hal-04661164
https://hal.science/hal-04661164v1

Submitted on 31 Oct 2024

HAL is a multi-disciplinary open access archive for the deposit and dissemination of scientific research documents, whether they are published or not. The documents may come from teaching and research institutions in France or abroad, or from public or private research centers.

L'archive ouverte pluridisciplinaire **HAL**, est destinée au dépôt et à la diffusion de documents scientifiques de niveau recherche, publiés ou non, émanant des établissements d'enseignement et de recherche français ou étrangers, des laboratoires publics ou privés.

Reduction of native singly ionized Zinc vacancies content by 2.5 MeV electron irradiation of $ZnGeP_2$ single crystals

C. Vernozy, A. Alessi, J. Petit, A. Courpron, O. Cavani, V. Véniard

C. Vernozy
DMAS/ONERA, Université Paris-Saclay, F-92322 Chatillon, France
LSI, CEA/DRF/IRAMIS, CNRS, Ecole polytechnique, Institut Polytechnique de Paris, 91120 Palaiseau, France

A. Alessi
LSI, CEA/DRF/IRAMIS, CNRS, Ecole polytechnique, Institut Polytechnique de Paris, 91120 Palaiseau, France

J. Petit
DMAS/ONERA, Université Paris-Saclay, F-92322 Chatillon, France

A. Courpron
LSI, CEA/DRF/IRAMIS, CNRS, Ecole polytechnique, Institut Polytechnique de Paris, 91120 Palaiseau, France

O. Cavani
LSI, CEA/DRF/IRAMIS, CNRS, Ecole polytechnique, Institut Polytechnique de Paris, 91120 Palaiseau, France

V. Véniard
LSI, CEA/DRF/IRAMIS, CNRS, Ecole polytechnique, Institut Polytechnique de Paris, 91120 Palaiseau, France

e-mail: antonino.alessi@polytechnique.edu, charlotte.vernozy-trouillet@onera.fr.

Keywords: irradiation effects, point defects, $ZnGeP_2$

Abstract. We present an experimental study on how to reduce the content of singly ionized zinc vacancy (V^-_{Zn}) in $ZnGeP_2$ crystals to improve their optical quality. Their EPR (electron paramagnetic resonance) signal has been studied in samples treated in different ways. Our data provide a scheme of the reductions that can be obtained by the different methods or by their combination. The adding of Sn during the synthesis phase helps the production of large sizes single crystals and the reduction of the content of V^-_{Zn}. Thermal treatment and electron irradiation are then needed to induce a further decrease. Up to 2×10^{17} e/cm^2, the kinetics of V^-_{Zn} content as a function of the fluence, do not feature a limit value, so larger reductions of V^-_{Zn} content may be possible.

1. Introduction

Zinc germanium diphosphide is a nonlinear optical crystal with remarkable properties for frequency conversion in the mid-IR [1]. Indeed, $ZnGeP_2$ (ZGP) has a very wide theoretical transparency band (0.74-12 µm) [2–4], a strong nonlinearity coefficient (75 pm/V) [4, 5] for frequency conversion and a high thermal conductivity (35 W/m/K) [3, 4], which are needed to work with high power beams [6, 7]. ZGP can be used in Optical Parametric Oscillators (OPO), which are powerful and tunable laser sources, based on the conversion of well-known 2 µm conventional laser sources [8–12]. The tunability of these OPOs is based on the use of nonlinear optical crystals with high birefringence for phase matching purposes [10]. The high power of these sources [12] allows the generation of light that can travel over long distances in the atmosphere (within mid-IR transparency bands). These sources can be used for applications such as long-range detection of gaseous species [4, 7, 13] by scanning the infrared thanks to their strong tunability. OPO laser sources can also be used for optronic countermeasures [4, 7], or surgery applications [4, 7, 14].

Nevertheless, to efficiently use ZGP in OPOs pumped at 2 µm, the absorption coefficient in the crystal must be as low as possible at that wavelength (below 0.15 cm^{-1} [15]), and ZGP exhibits a near-band optical absorption, which is overlapping with the OPO pumping wavelength [16–18]. Generally, as-grown ZGP crystals exhibit an absorption coefficient of 0.3 to 1 cm^{-1} at 2 µm. This optical absorption is caused by point defects [19, 20], due to small deviations of the stoichiometry during the growth process [7, 20–22]. These point defects are present in high concentration in all as-grown ZGP crystals, and studies have identified at least three paramagnetic centers : the neutral phosphorus vacancy (V^0_P) [23] and the germanium-on-a-zinc

antisite (Ge_{Zn}^{+}) [24] which are both donors, and the singly ionized vacancy (V^{-}_{Zn}) [25] which is the dominant acceptor.

On the one hand, according to [26], the absorption band in the 0.9–2.5 µm region could be caused by Ge substituting Zn. On the other hand, according to [17], the optical absorption near-edge can be decomposed in three distinct bands peaking at 1.2, 2.2 and 2.3 µm, with tails overlapping one another and the V^{-}_{Zn} centers should be responsible for both 1.2 and 2.2 µm absorption bands, whereas V_P should be responsible for the 2.3 µm band [17].

A great number of studies have shown that the zinc vacancy defect content in the crystal is connected with the optical absorption, as crystals with a high V^{-}_{Zn} content exhibit large absorption coefficient and low defect content crystals have a good optical transparency around 2 µm [21, 27–31].

V^{-}_{Zn} is present in all bulk $ZnGeP_2$ crystal and can easily be detected by Electron Paramagnetic Resonance (EPR) spectroscopy without photoexcitation at low temperature [25, 32]. When the magnetic field (B) is parallel to the crystallographic c axis ([001]) of ZGP, the EPR spectrum of V^{-}_{Zn} consists of three lines. These lines are the result of hyperfine interactions of the unpaired electron with two equivalent P nuclei. More in details, V^{-}_{Zn} has four equivalent orientations in the lattice when B is parallel to [001], and the signal results in an overlapping of the four triplet spectra, which gives rise to the spectrum of a more simple triplet system with a relative ratio of 1:2:1 [25, 32].

The concentration of V^{-}_{Zn} in the material is related to its corresponding EPR spectrum intensity [33]. Therefore, the EPR spectrum intensity of zinc vacancies is directly related to the optical absorption around 2 µm in ZGP [21].

A common method to reduce the absorption coefficient of ZGP at 2 µm, as well as the V^{-}_{Zn} content in the crystal, is a post-growth thermal annealing [1]. This treatments allows to reduce both ZGP absorption coefficient and V^{-}_{Zn} content by roughly 50 % [20, 34–36]. The most efficient annealing parameters are a temperature of 500-600 °C for a 300-600 h treatment with ZGP powder [20, 34, 35]. However, in most cases, a post-growth annealing is not enough to obtain the required level of transmission at 2 µm for OPO applications.

Therefore, it was found that e-beam or γ-rays irradiation of ZGP crystals allow to further reduce both the 2 µm optical absorption coefficient and the V^{-}_{Zn} content [26, 28, 37–40], a process that we can call bleaching. The irradiation is usually performed at 2 to 5 MeV [41–43] and its effect on both the V^{-}_{Zn} content and the optical absorption can be stronger than the annealing. So, combining effect of both thermal annealing and irradiation allow to produce ZGP of good optical quality to be used in OPOs [12, 34, 43].

Moreover, first results on tin (Sn) addition in ZGP crystals were published in a patent [44], and the author showed that adding Sn is an efficient way to reduce the 2 µm absorption of as-grown and annealed crystals.

In this work, we will focus on the study of the singly ionized zinc vacancy acceptor, as it is an optically active defect, closely related to the optical absorption in $ZnGeP_2$. We investigated the V^-_{Zn} content by EPR in samples produced and post-treated with different procedures and process parameters. Electron beam irradiations on crystals were performed at various temperatures and fluences, to monitor the changes in V^-_{Zn} content in correlation with the sample post-treatments. The reported set of data allowed to identify the treatment needed to obtain a certain level of V^-_{Zn} content reduction. The most efficient way to obtain large size single crystals with low content of V^-_{Zn} is the irradiation of thermally annealed material produced by adding Sn. It is also important to note that irradiation with fluence higher than 2×10^{17} e/cm^2 could improve the bleaching of this defects.

2. Experimental details

Synthesis has been carried out by the two zone process [45]. High purity (5 or 6 N) Zinc (Zn), Germanium (Ge), Phosphorus (P), and eventually tin (Sn) chunks have been introduced in an evacuated (10^{-5} mbar) quartz ampoule as a reactor. Excesses of Zn and P have also been added to minimize deviation from stoichiometry resulting from the compounds volatility [2]. The reactor has then been put in a two-zone tube furnace, whose axis is tilted by 15° from the horizontal direction, to control the pressure in the sealed reactor from P evaporation. The remaining Ge and Zn (and Sn), mainly in the molten state when temperature increases, stay in the lowest part which is the hottest (up to 1050°C), whereas the P vapor stays in the highest part of the reactor which is colder (500°C), thus limiting its pressure. The reactor and the furnace have been placed in a steel chamber. Inside, an argon pressure of 10 bars has been applied outside the ampoule to limit the risk of reactor explosion. After a few hours, when the chemical reaction has consumed a large part of the phosphorus, the upper zone temperature has been slowly raised (up to 1080°C) in order to consume the remaining P vapor. The temperature was maintained for 40 hours in the reactor before cooling down to 800°C at 0.3°C/min, then to room temperature at 3°C/min. Table 1 summarizes the starting compositions used to produce the investigated samples.

The crystal growth step has been carried out by the Vertical Bridgman method [43] in a furnace from the Cyberstar-ECM company. Previously synthetized $ZnGeP_2$ compound has been

grinded and introduced in a pyrolytic boron nitride crucible before being put inside an evacuated (10^{-5} mbar) quartz ampoule. A single-crystal seed can be inserted at the tip of the crucible to help the crystal growth. The material has been grown by pulling the ampoule through a temperature gradient (~15 °C/cm near the melting point at 1030°C) at a rate of 0.4 mm/h. Ingots from 60g to 100g (Ø25 mm) were processed.

All ingots were polycrystalline as the precise control of the temperature near the seed is difficult, however large single crystals have been obtained and especially by adding Sn during the synthesis phase. Preliminary Energy Dispersive X-ray spectroscopy (EDX) investigations indicate that the great part of the Sn segregates out of the crystals.

Table 1. Molar content of Zn, Ge, P and Sn in investigated samples of ZGP and ZGP with an addition of Sn (ZGP/Sn).

	ZGP	ZGP/Sn
Zn (m%)	0.331	0.327
Ge (m%)	0.356	0.352
P (m%)	0.313	0.310
Sn (%m)	0	0.012

After growth, some of the samples have been annealed. The samples were put inside a closed vacuum quartz ampoule with additional $ZnGeP_2$ powder. Table 2 summarizes the thermal annealing conditions applied on the different investigated samples.

Table 2. Sample identification, temperature and duration of the annealing thermal treatment.

	ZGP66	ZGP83*	ZGP88	ZGP90	ZGP/Sn92	ZGP/Sn92TT
Temperature	550 °C	550 °C	-	550 °C	-	550 °C
Time	600 h	500 h	-	600 h	-	550 h

* This material was submitted to three crystal growth processes

Electron irradiations have been performed at SIRIUS, a Pelletron electron accelerator produced by NEC [46]. It can generate electron beams with energies in the range 150 keV - 2.5 MeV and currents in the range 10 nA - 50 µA. The beam line operates under vacuum, at 5×10^{-8} mbar, to avoid degradation of the beam energy and current before its impact on the sample. SIRIUS

is equipped with several irradiation cells and the irradiation can be performed in different conditions [47]. Every irradiation test reported in the present investigation has been performed with the irradiation cell named Cirano using a beam energy of 2.5 MeV. According to ESTAR [48], at 2.5 MeV the stopping powers of Zn, Ge and P are between 1.3 and 1.5 MeVcm^2/g, so we can reasonably assume that the stopping power of $ZnGeP_2$ is about 1.4 MeVcm^2/g and we can evaluate a maximum dose of about 45 MGy. The investigated irradiation conditions are reported in Table 3. The ZGP66 sample purpose was to investigate the irradiation temperature and flux effect on the V^-_{Zn} content. All the other samples were irradiated at room temperature with various fluences to investigate the effect on the V^-_{Zn} content, depending on the samples post-treatment.

Table 3 : 2.5 MeV Irradiation parameters of investigated samples.

	ZGP66	ZGP83 ZGP88 ZGP90 ZGP/Sn92 ZGP/Sn92TT
Fluence (e/cm^2)	2×10^{17}	1×10^{15} to 2×10^{17}
Flux (e/(cm^{2}s))	10^{13} and 10^{12}	10^{13}
Temperature (K)	290 to 690	290

All samples were investigated by EPR using a Jeol JES-X310 spectrometer working in X-band with a modulation frequency of 100 kHz. The data were recorded at 123 K (and in some cases at 300 K) employing the Jeol DVT control system. All spectra were recorded with power in the linear part of the saturation curve. Spectra of different samples were compared after normalization to both the sample mass and the parameters of the measurement.

3. Results

The EPR signal was recorded before irradiation for all investigated samples. By comparing the intensities of the V^-_{Zn} EPR spectra, we found the highest V^-_{Zn} content in the as-grown sample ZGP88. In samples produced by adding Sn (ZGP/Sn92) the V^-_{Zn} content was reduced by 50% compared to ZGP88. After being annealed (ZGP90), the V^-_{Zn} content was reduced by 60-70% compared to the as-grown material (ZGP88). In ZGP83 sample the EPR signal of V^-_{Zn} is about 50% the one of ZGP88. In samples produced by adding Sn, after annealing (ZGP/Sn92TT), the

V^{-}_{Zn} content was reduced by 70% compared to the as-grown ZGP88. This data will be summarized in the discussion section together with the irradiation effects.

Figure 1 shows the EPR spectra of V_{Zn}^{-} in ZGP66 samples irradiated under various temperatures in the range 290-690 K at fluence 2 $\times 10^{17}$ e/cm^2. The spectra were recorded at 123 K with the magnetic field parallel to the c crystallographic axis ([001]).

By comparing the intensities of the signals recorded in samples before (black curve) and after irradiation at various temperatures, we note that irradiations at room temperature are more efficient in bleaching this kind of defects than irradiations at high temperature. Indeed, the ratio of the sample prior to irradiation (black curve) to the sample irradiated at 300 K (blue curve) is about 6, while the ratio of the sample prior to irradiation (black curve) to the sample irradiated at 690 K (red curve) is about 2. Consequently, further investigations were done with irradiations at room temperature. By comparing samples irradiated at room temperature, but with different fluxes (blue and magenta curves), we do not observe significant difference in the V_{Zn}^{-} EPR spectra intensities.

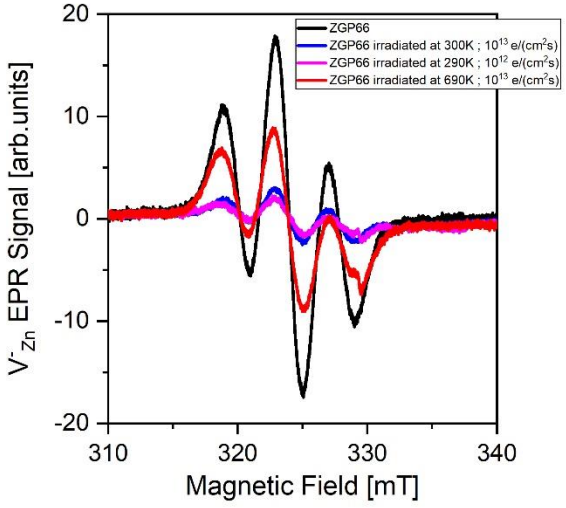

Figure 1. Experimental EPR spectra of V^{-}_{Zn} in electron irradiated samples from ZGP66 ingot at various irradiation temperature for magnetic field B parallel to the c crystallographic axis.

Figure 2 shows the change of intensity of the V^{-}_{Zn} signal in a ZGP66 sample (irradiated up to 2 $\times$ 10^{17} e/cm^2 at 300 K) as a function of the post-irradiation annealing time. The data show that post-irradiation treatments at 423K with duration between 2000 and 12000 seconds induce an increase of the V^{-}_{Zn} defect content of at least 50%, which implies the loss of part of the positive effects induced by irradiation.

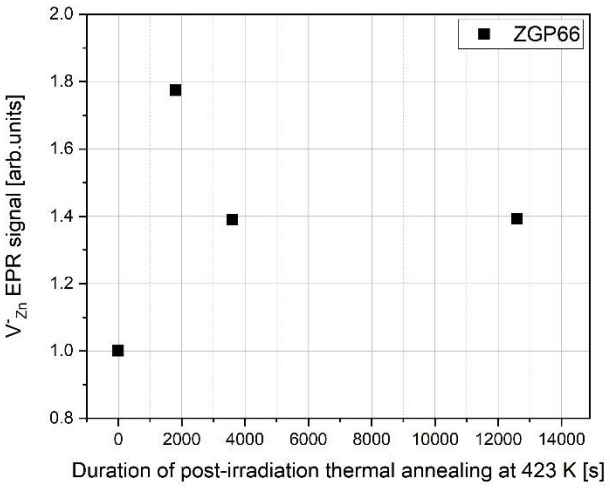

Figure 2. EPR intensity of V^-_{Zn} spectra as a function of the annealing time at 423 K in ZGP66 sample after irradiation at a fluence of 2×10^{17} e/cm^2 (at 300 K).

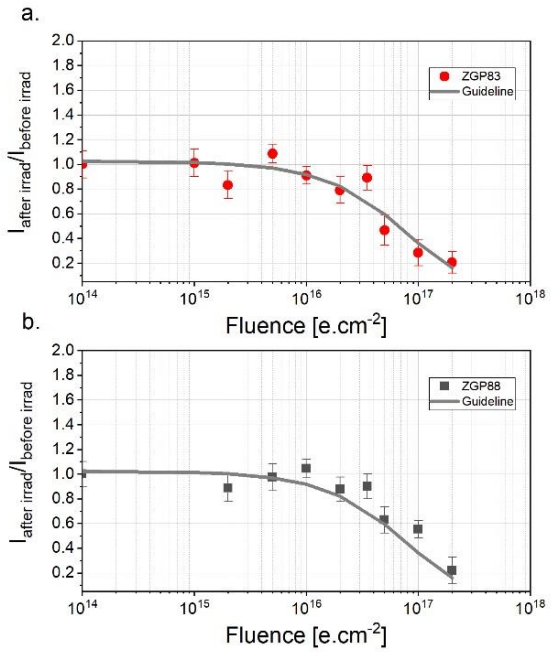

Figure 3. Ratio of experimental EPR spectra intensities of V^-_{Zn} after irradiation to the ones before irradiation as a function of the fluence in ZGP83 samples (a) and ZGP88 samples (b); a gray line is reported as guideline of the kinetics.

Figures 3.a (for ZGP83) and 3.b (for ZGP88) show the ratio of the intensities of the V^-_{Zn} EPR signal after (I_{after}) to the ones before (I_{before}) irradiation as a function of the fluence. We note that both kinetics are similar, and we use the same curve as guideline in both graphs. For both samples the V^-_{Zn} concentration is stable up to about 2×10^{16} e/cm^2, although it seems to start

decreasing a little bit later in the as-grown sample (see Figure 3b sample ZGP88). At the maximum investigated fluence (2×10^{17} e/cm^2), the V^-_{Zn} concentration is about 5 times lower than the one measured before irradiation in both samples. In the annealed samples (ZGP83) the decreasing rate seems to start slowing down at the highest fluence investigated.

Figure 4 illustrates the kinetics of the V^-_{Zn} EPR signals as a function of the fluence, recorded in the samples produced by adding Sn. The guideline curve (grey) is the same as the one reported in figure 3. We note that the kinetics observed for ZGP88 and ZGP83 are very similar. However, the decrease seems to start later, at a higher fluence in the case of ZGP/Sn92. As for the other samples, in both ZGP/Sn92 and ZGP/Sn92TT the V^-_{Zn} EPR intensity went through a reduction of about a factor 5 at the highest fluence (2×10^{17} e/cm^2). In all cases the kinetics do not reach a saturation minimum value, so further bleaching could be possible at higher fluence.

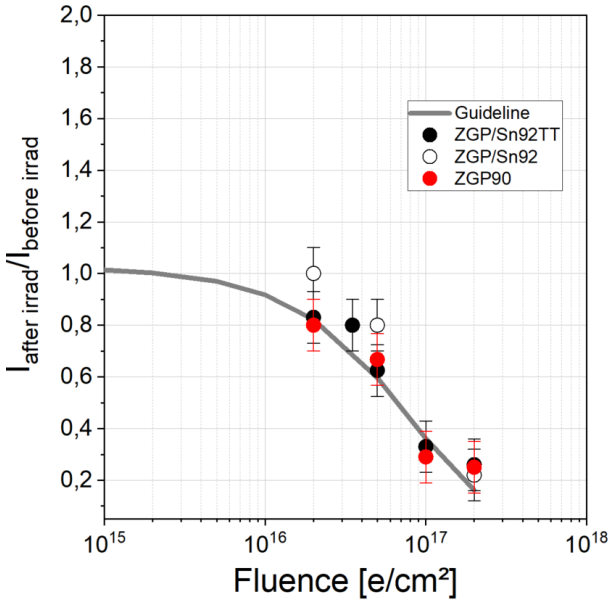

Figure 4. Ratio of experimental EPR spectra intensity of V^-_{Zn} after irradiation to prior irradiation as a function of the fluence in: ZGP/Sn92TT (annealed), ZGP/Sn (as-grown) and ZGP90 (annealed).

4. Discussion

The comparison of the data recorded before irradiation shows that the addition of Sn is an efficient method to decrease the content of the V^-_{Zn} acceptor, while thermal annealing requires high temperature and a long time to achieve the bleaching of this type of defects.

Irradiation with electrons shows an attractive ability of reducing the content of the V^-_{Zn}. In fact, the data of Figure 1, Figure 3 and Figure 4, show that samples go through a drop of V^-_{Zn}

concentration of a factor about 5 at fluence 2×10^{17} e/cm^2. The data highlight that the increase of the irradiation temperature does not improve the bleaching of the defects, but on the contrary, limits the positive effect of the irradiation.

Since the kinetics of the bleaching of V^{-}_{Zn} can depend on the starting defect content, we investigated the fluence effect on different samples. The data of Figure 3b suggest that it is possible to induce an efficient bleaching of the V^{-}_{Zn} in the samples even when they are not previously thermally annealed after growth. In fact, although in as-grown ZGP (ZGP88) the content of these defects is about twice larger than in annealed ZGP (ZGP83), the kinetics is similar and a reduction of a factor 5 of the V^{-}_{Zn} is observed after irradiation at fluence 2×10^{17} e/cm^2. In addition, we note that an irradiation at a fluence of 1×10^{17} ecm^{-2} (3h of irradiation with flux 10^{13} e/(cm^{2}s)) is able to reduce of about a factor 2 the V^{-}_{Zn} content in ZGP88, which is comparable to what is obtained with thermal treatment or with Sn addition on as-grown samples.

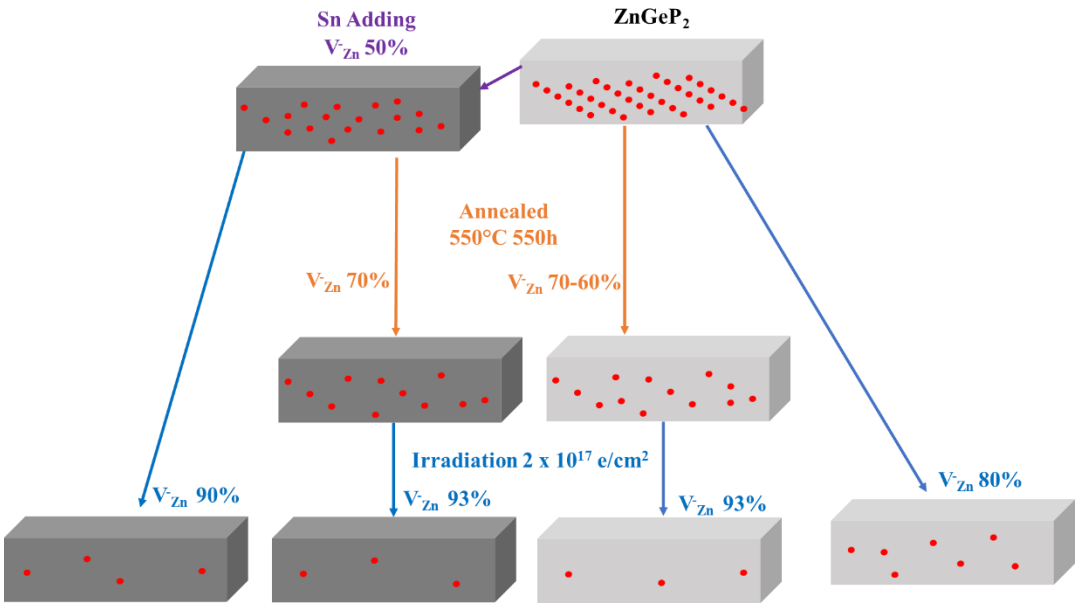

Figure 5. Summary of various ways to reduce the V^{-}_{Zn} in ZGP, all the values are the percentage of reduction with respect to the ZGP as-grown sample.

Since the use of Sn during the synthesis phase is able to reduce the starting content of the defects, we also tested the irradiation effects on that type of samples. As reported in Figure 4, the kinetics are comparable to the ones observed in the other samples. In fact, the irradiation still reduces the V^{-}_{Zn} content of about a factor 5 in ZGP/Sn92 and ZGP/Sn92TT. Only minor differences are observed.

Figure 5 summarizes the different reductions obtained with different methods or their combinations. Irradiation at high temperature is not reported since the positive effect is limited

to a decrease of the signal of a factor ~2, compared to an irradiation at room temperature (300 K), where the V^-_{Zn} content reduction is of a factor ~6. For similar reasons in Figure 5 we do not report the method which suggests a post-irradiation thermal treatment, as it deletes part of the bleaching induced by irradiation, and re-increases the V^-_{Zn} content in the sample.

For each sample, the kinetics does not reach a minimum value so it seems possible to increase the fluence to induce further bleaching of the V^-_{Zn}. However, as electron irradiation can induce displacement damage processes, it cannot be excluded that above a certain fluence value a significant amount of Zn vacancies can be created and that this mechanism interferes with their bleaching. It is also important to note that by reaching a high level of V^-_{Zn} bleaching, the presence of other minor contributions to the absorption at 2 μm could emerge (for example due to other defects).

It is interesting to compare our data with previous investigations focused on electron and γ irradiations. In ref [39] the authors observed a decrease of about a factor 3.5 after γ-rays irradiations with doses equivalent to those of 2.5 MeV electrons with fluences between 0.5×10^{18} and 1×10^{18} e/cm^2 at a temperature of about 373 K. Such data are in quite good agreement with ours, considering that the increase of the irradiation temperature tends to decrease the degree of V^-_{Zn} bleaching.

Since γ-rays are not as efficient as electrons in inducing displacement damage processes it seems reasonable to suggest that the observed bleaching is related to ionizing dose effects. Considering other electron irradiation investigations [41], [49], the bleaching can be attributed to a charge change of the V^-_{Zn}. It can be seen as a charge exchange with the induced defects or as a shift of Fermi level due to the induced defects.

5. Conclusion

The intensity of the EPR signal of the singly ionized zinc vacancy has been investigated in as-grown, annealed and electron irradiated materials, as well as in samples produced by adding Sn. The combination of adding Sn in the synthesis phase, annealing and electron irradiation appears to be the best to obtain single crystals of large sizes with the lowest V^-_{Zn} content. Since we considered different methods of bleaching, the present investigation can be used to select the easiest path that allows a specific required reduction of V^-_{Zn}.

Reference

[1] P. G. Schunemann, K. T. Zawilski, L. A. Pomeranz, D. J. Creeden, P. A. Budni, *J. Opt. Soc. Am. B* **2016**, *33*, D36.

[2] J. L. Shay, J. H. Wernick, *Ternary Chalcopyrite Semiconductors: Growth, Electronic Properties, and Applications*, Pergamon Press, Oxford, New York **1975**.

[3] D. N. Nikogosian, *Nonlinear Optical Crystals: A Complete Survey*, Springer-Science, New York **2005**.

[4] K. L. Vodopyanov, *Laser-based Mid-infrared Sources and Applications*, Wiley **2020**.

[5] G. D. Boyd, E. Buehler, F. G. Storz, *Appl. Phys. Lett.* **1971**, *18*, 301–304.

[6] J. Cheng, S. Zhu, B. Zhao, B. Chen, Z. He, Q. Fan, T. Xu, *J. Cryst. Growth* **2013**, *362*, 125–129.

[7] Z. Lei, C. Zhu, C. Xu, B. Yao, C. Yang, *J. Cryst. Growth* **2014**, *389*, 23–29.

[8] P. A. Budni, P. G. Schunemann, M. G. Knights, T. M. Poliak, E. P. Chicklis, in *Advanced Solid State Lasers*, OSA, Santa Fe, New Mexico **1992**, pp. 380–383.

[9] A. Hemming, J. Richards, A. Davidson, N. Carmody, S. Bennetts, N. Simakov, J. Haub, *Opt. Express* **2013**, *21*, 10062.

[10] S. Das, *Opt Quant Electron* **2019**, *51*, 70.

[11] A. I. Gribenyukov, V. V. Dyomin, A. S. Olshukov, S. N. Podzyvalov, I. G. Polovtsev, N. N. Yudin, *Russ Phys J* **2019**, *61*, 2042–2052.

[12] N. N. Yudin, O. L. Antipov, A. I. Gribenyukov, I. D. Eranov, S. N. Podzyvalov, M. M. Zinoviev, L. A. Voronin, E. V. Zhuravleva, M. P. Zykova, *Quantum Electron.* **2021**, *51*, 306–316.

[13] A. A. Ionin, I. O. Kinyaevskiy, A. A. Kotkov, D. V. Sinitsyn, Y. M. Andreev, *Appl Spectrosc* **2022**, *76*, 1504–1512.

[14] G. Stoeppler, M. Eichhorn, M. Schellhorn, S. L. Been, R. M. Verdaasdonk, **2012**.

[15] A. I. Gribenyukov, *Atmos. Oceanic Opt.* **2002**, *15*, 61–68.

[16] E. Buehler, J. H. Wernick, J. D. Wiley, *J. Electron. Mater.* **1973**, *2*, 445–454.

[17] N. C. Giles, L. Bai, M. M. Chirila, N. Y. Garces, K. T. Stevens, P. G. Schunemann, S. D. Setzler, T. M. Pollak, *J. Appl. Phys.* **2003**, *93*, 8975–8981.

[18] H. Xie, S. Fang, H. Zhao, X. Xu, N. Ye, W. Zhuang, *RSC Adv.* **2019**, *9*, 35771–35779.

[19] K. S. Titov, V. N. Brudnyi, *Russ Phys J* **2014**, *57*, 50–54.

[20] G. A. Verozubova, A. O. Okunev, A. I. Gribenyukov, *J. Cryst. Growth* **2014**, *401*, 782–786.

[21] N. C. Giles, L. E. Halliburton, *MRS Bull.* **1998**, *23*, 37–40.

[22] G. A. Verozubova, A. I. Gribenyukov, V. V. Korotkova, A. W. Vere, C. J. Flynn, *J. Cryst. Growth* **2002**, *237–239*, 2000–2004.

[23] N. C. Giles, L. E. Halliburton, P. G. Schunemann, T. M. Pollak, *Appl. Phys. Lett.* **1995**, *66*, 1758–1760.

[24] S. D. Setzler, N. C. Giles, L. E. Halliburton, P. G. Schunemann, T. M. Pollak, *Appl. Phys. Lett.* **1999**, *74*, 1218–1220.

[25] K. T. Stevens, S. D. Setzler, L. E. Halliburton, N. C. Fernelius, P. G. Schunemann, T. M. Pollak, *MRS Proc.* **1997**, *484*, 549.

[26] A. I. Gribenyukov, G. A. Verozubova, A. Yu. Trofimov, A. W. Vere, C. J. Flynn, *MRS Proc.* **2002**, *744*, M5.40.

[27] S. D. Setzler, L. E. Halliburton, N. C. Giles, P. G. Schunemann, T. M. Pollak, *MRS Proc.* **1996**, *450*, 327.

[28] V. N. Brudnyi, D. L. Budnitskii, M. A. Krivov, R. V. Masagutova, V. D. Prochukhan, Yu. V. Rud, *Phys. Stat. Sol. (a)* **1978**, *50*, 379–384.

[29] P. Zapol, R. Pandey, M. Ohmer, J. Gale, *J. Appl. Phys.* **1996**, *79*, 671.

[30] N. C. Giles, L. E. Halliburton, P. G. Schunemann, in (Eds.: G.J. Quarles, L. Esterowitz, L.K. Cheng), San Jose, CA **1995**, pp. 175–184.
[31] G. Medvedkin, *J. Opt. Soc. Am. B* **2022**, *39*, 851.
[32] M. H. Rakowsky, W. K. Kuhn, W. J. Lauderdale, L. E. Halliburton, G. J. Edwards, M. P. Scripsick, P. G. Schunemann, T. M. Pollak, M. C. Ohmer, F. K. Hopkins, *Appl. Phys. Lett.* **1994**, *64*, 1615–1617.
[33] J. Möser, K. Lips, M. Tseytlin, G. R. Eaton, S. S. Eaton, A. Schnegg, *J. Magn. Reson.* **2017**, *281*, 17–25.
[34] D.-H. Yang, B.-J. Zhao, B.-J. Chen, S.-F. Zhu, Z.-Y. He, Z.-R. Zhao, M.-D. Liu, *Mater. Sci. Semicond. Process.* **2017**, *67*, 147–151.
[35] H.-G. Ang, L.-L. Chng, Y.-W. Lee, C. J. Flynn, P. C. Smith, A. W. Vere, *MRS Proc.* **1999**, *607*, 433.
[36] P. G. Schunemann, T. M. Pollak, *MRS Bull.* **1998**, *23*, 23–27.
[37] P. G. Schunemann, P. J. Drevinsky, M. C. Ohmer, W. C. Mitchel, N. C. Fernelius, *MRS Proc.* **1994**, *354*, 729.
[38] P. G. Schunemann, P. J. Drevinsky, M. C. Ohmer, *Mat. Res. Soc. Symp. Proc.* **1995**, *354*, 5.
[39] M. H. Rakowsky, W. J. Lauderdale, R. A. Mantz, R. Pandey, P. J. Drevinsky, *MRS Proc.* **1994**, *354*, 735.
[40] S. V. Chuchupal, G. A. Komandin, E. S. Zhukova, O. E. Porodinkov, I. E. Spektor, A. I. Gribenyukov, *Phys. Solid State* **2015**, *57*, 1607–1612.
[41] W. Gehlhoff, D. Azamat, A. Hoffmann, N. Dietz, *J. Phys. Chem. Solids* **2003**, *64*, 1923–1927.
[42] G. A. Verozubova, A. I. Gribenyukov, A. W. Vere, C. J. Flynn, Yu. F. Ivanov, in Vol. 607, Material Research Society **1999**, pp. 457–463.
[43] A. I. Gribenyukov, *Preparation of ZnGeP2 for Nonlinear Optical Applications : Melt And Homoepitaxial Vapor Growth, Properties Of The Grown Crystals*, Institute For Optical Monitoring Of Siberian Division Of The RAS, Tomsk, 634021, RUSSIA **2001**.
[44] R. J, P. J, 1402220, **2015**.
[45] G. A. Verozubova, A. I. Gribenyukov, Y. P. Mironov, *Inorganic Materials* **2007**, *43*, 1040–1045.
[46] National Electrostatic Corp., "National Electrostatic Corp.," available at https://www.pelletron.com/, **n.d.**
[47] Laboratoire des solides irradiés, "L'installation SIRIUS," available at https://portail.polytechnique.edu/lsi/fr/equipements/linstallation-sirius, **n.d.**
[48] NIST Physical Measurement Laboratory, "ESTAR program," available at https://physics.nist.gov/PhysRefData/Star/Text/ESTAR.html, **n.d.**
[49] A. Hoffmann, H. Born, A. Näser, W. Gehlhoff, J. Maffetone, D. Perlov, W. Ruderman, I. Zwieback, N. Dietz, K. J. Bachmann, *MRS Proc.* **1999**, *607*, 373–378.